Robust scheduled control of longitudinal flight with handling quality satisfaction

D. Saussié
david.saussie@polymtl.ca
Department of Electrical Engineering
École Polytechnique de Montréal
Montréal, Canada

C. Bérard
Department of Mathematics, Computer Science and Control Theory
ISAE
Toulouse, France

O. Akhrif
Department of Electrical Engineering
École de Technologie Supérieure
Montréal, Canada

L. Saydy
Department of Electrical Engineering
École Polytechnique de Montréal
Montréal, Canada

ABSTRACT

Classic flight control systems are still widely used in the industry because of acquired experience and good understanding of their structure. Nevertheless, with more stringent constraints, it becomes difficult to easily fulfil all the criteria with these classic control laws. On the other hand, modern methods can handle many constraints but fail to produce low order controllers. The following methodology proposed in this paper addresses both classic and modern flight control issues, to offer a solution that leverages the strengths of both approaches. First, an H_∞ synthesis is performed in order to get controllers which satisfy handling qualities and are robust with respect to mass and centre of gravity variations. These controllers are then reduced and structured by using robust modal control techniques. In conclusion, a self-scheduling technique is described that will schedule these controllers over the entire flight envelope.

NOMENCLATURE

Drb	Gibson's dropback
g	acceleration due to gravity, ms^{-1}
h	altitude, ft
l_x	distance between the accelerometer and the centre of gravity, m
m	mass, lbs
M	Mach number
n_z	normal load factor, g's
q	pitch rate, rad/s
q	dynamic pressure, lb/ft^2
U_0	trimmed longitudinal speed, s
w	normal velocity perturbation, ms^{-1}
x_{cg}	centre of gravity location, (% of the chord)
δ_e	elevator angle deflection, rad
$\in$	tail downwash angle, rad
ζ_{sp}	short period damping
IRU	inertial reference unit
ST	settling time, s

1.0 INTRODUCTION

Developing, flight-testing and integrating flight control systems is costly and time-consuming. Modern techniques such as H_∞ or μ-synthesis provide effective and robust controllers, but the main problem remains their high order which prevents them from being easily implemented[1,2]. Classical flight control systems are still widely used because of their well-studied and understood archi-

Paper No. 3605. Manuscript received 28 June 2010, revised version received 29 September, 2010 accepted 15 November 2010.

https://doi.org/10.1017/S000192400000556X Published online by Cambridge University Press

tecture[3]. However, these systems must deal with stringent performance and robustness requirements over the full flight envelope.

In this paper, we propose a comprehensive methodology that establishes a flight controller for the longitudinal flight of a business jet aircraft, namely Challenger 604. This methodology is based on techniques that have been proven successful separately. First, H_∞ synthesis[4,5] is performed to find high order controllers that satisfy handling quality requirements and have robustness property with respect to some parameters. Obviously, H_∞ controllers cannot be implemented because of their order. They have to be reduced sufficiently without losing performance. If classic reduction methods[6] often fail to produce very low order controllers, modal reduction[7] (inspired by robust modal control[8,9]) usually succeeds in that task. Finally, in order to have a controller efficient and robust on the entire flight envelope, a self-scheduling technique[10] is used. Contrary to classic gain-scheduling[11,12] where the controllers are interpolated a posteriori with respect to scheduling variables, the controller interpolation can be chosen *a priori*.

The paper is organised as follows. Theoretical backgrounds are provided in Section 2 about robust modal control. The aircraft model of Challenger 604 is presented in Section 3 as well as handling qualities of interest. Section 4 is devoted to the application of our design methodology: first H_∞ synthesis is performed, then a reduction method based on robust modal control is applied to these controllers and finally, scheduling of the controller with respect to dynamic pressure $\bar{q}$ and altitude h is done.

2.0 ROBUST MODAL CONTROL

2.1 Notations

Consider a linear time invariant (LTI) system with n states, m inputs and p outputs written in state-space form;

$$\dot{x} = A(\Delta)x + B(\Delta)u \quad \ldots (1)$$

$$y = C(\Delta)x + D(\Delta)u \quad \ldots (2)$$

where x is the state vector, u the input vector, y the output vector and Δ the uncertain parameter matrix. The state-space matrices $A \in \mathbb{R}^{n\times n}$, $B \in \mathbb{R}^{n\times m}$, $C \in \mathbb{R}^{p\times n}$ and $D \in \mathbb{R}^{p\times m}$ depend on Δ. In this paper, we will suppose that we have a bank of models $\{M_j=(A_j,B_j,C_j,D_j), j = 1\ldots r\}$ obtained for different values $\Delta = \Delta_j$ of the parameters.

2.2 Eigenstructure assignment

Proposition 1 from Le Gorrec[13] generalises the traditional eigenstructure assignment of Moore[14] for the use of dynamic controllers.

Proposition 1. The triplet $T_i = (\lambda_i, v_i, w_i) \in \mathbb{C}\times \mathbb{C}^n \times \mathbb{C}^m$ satisfying

$$\begin{bmatrix} A-\lambda_i I & B \end{bmatrix}\begin{bmatrix} v_i \\ w_i \end{bmatrix} = 0 \quad \ldots (3)$$

is assigned by the dynamic gain $K(s)$ if and only if;

$$K(\lambda_i)(Cv_i + Dw_i) = w_i \quad \ldots (4)$$

If the eigenvalue is complex, Equation (4) has to be completed by its conjugate;

$$K(\bar{\lambda}_i)(C\bar{v}_i + D\bar{w}_i) = \bar{w}_i \quad \ldots (5)$$

The input direction w_i and right eigenvector v_i associated with the closed-loop eigenvalue λ_i can be fixed by various methods (e.g. decoupling objectives, orthogonal projection of open-loop eigenvector).

The elementary design procedure associated with this proposition is as follows:

- Choose a set of auto-conjugate closed-loop eigenvalues λ_i and determine the closed-loop admissible eigenvector space using Equation (3). At this step, the triplets $T_i = (\lambda_i, v_i, w_i)$ are defined.
- Compute $K(s)$ satisfying Equation (4). This computation is detailed in the next section for the multi-model modal control but this would apply for the single-model modal control as well.

2.3 Multi-model modal control

Multi-model eigenstructure assignment[15] is done by simultaneously assigning triplets T_i for several models, which reduces to solve a set of equality constraints of type Equation (4). The choice of the models to treat with and the triplets to assign is determined by an analysis of the stability and/or performance robustness. The feedback controller $K(s)$ is considered here in a transfer matrix form. The purpose of this section is to find a dynamic controller that solves the set of linear constrains of the form (Equation (3)) and (Equation (4)). The transfer matrix of the controller will be composed of $p \times m$ rational functions at each input/output:

$$K_{ij}(s) = \frac{b_{ijq}s^q + \cdots + b_{ij1}s + b_{ij0}}{a_{ijq}s^q + \cdots + a_{ij1}s + a_{ij0}} \quad \ldots (6)$$

Common or different denominators $D_{ij}(s)$ of the matrix $K(s)$ are fixed a priori with a sufficiently high order to realise the desired 'roll-off'. Furthermore, its degree must be chosen in order to offer enough numerator coefficients b_{ijk}, the tuning parameters (degrees of freedom). Generally, this choice offers too many degrees of freedom for the resolution of the equality constraints so that the problem is solved by minimising a criteria of type $J = \|K(s) - K_{ref}(s)\|$ over a certain frequency interval ω_i where $K_{ref}(s)$ is a reference controller (often a simple gain) synthesised for an initial model M_0. This reduces to minimising a quadratic criterion under linear constraints:

Proposition 2. The problem of computing $K(s)$ satisfying Equation (4) and minimising criterion J consists in solving for Ξ a *LQP* problem of the form;

$$\min J = \Xi H \Xi^T + 2\Xi c \quad \ldots (7)$$

$$s.t.\ \Xi A_1 = b_1 \quad \ldots (8)$$

where Ξ denotes unknown stacked coefficients of the numerators $b_{ij}k$. See Magni[15] for the theoretical background and further details, as well for software implementation. The procedure used in the following will be called (Mu-μ)-iteration.

Procedure 1. (Mu-μ)-iteration

Step A.1 – Elaborate a first initial design on a nominal model. All kinds of synthesis methods can be applied at this step (H_∞ control[4], LQG optimal control[16], μ-synthesis[17], etc...). In the case of initial non-modal approaches, look for eigenstructure assignment having the same characteristics as the initial controller.

Step B.1 – Proceed to a multi-model analysis of the pole map and/or time-responses and/or real μ-analysis[18,19]. If the initial design is satisfactory for all models or all values of uncertainties, then stop. Otherwise identify the worst-case model, determine its critical triplet T_i, and continue with **Step B.2**.

Step B.2 – Improve the behaviour of the worst-case model by replacing the triplet T_i by T_i* respecting the specifications while preserving the properties of all models treated before. Return to **Step B.1**.

Remark: See Magni[20] and Le Gorrec[13] for some general rules on multi-model eigenstructure assignment. For example to avoid

https://doi.org/10.1017/S000192400000556X Published online by Cambridge University Press

incompatible assignments one should treat models as 'far' as possible from each other in the considered parameter space and/or relax some constraints on models treated before.

This procedure can now be efficiently used for two purposes of interest, namely controller reduction and scheduling.

2.4 Modal reduction

We describe here how to combine modal analysis and dynamic eigenstructure assignment to reduce an initial controller while concurrently satisfying the closed-loop performances[7]. This method is based on the fact that the system is entirely defined by its closed-loop eigenstructure. First the dominant eigenstructure is extracted using modal analysis. In the second step, the dominant eigenstructure of the system will be assigned using a reduced order controller which has a fixed structure obtained from the first step of the procedure. Frequency criteria will be minimised to optimise the efficiency of the reduction.

Procedure 2. Modal Reduction

Step 1 – Modal analysis. For this purpose, modal simulation of the system controlled by the initial feedback is used, i.e. each mode is simulated separately[21]. From this kind of simulation, the contribution of each eigenvalue is evaluated. Only the eigenvalues (and associated eigenvectors) whose contribution is relevant are selected. This subset of eigenvalues/eigenvectors constitutes the dominant eigenstructure of the initial closed-loop system.

Step 2 – Reduction synthesis

- Choice of the controller poles: the choice is made *a priori* as a subset of the poles of the original controller. The selection is made using the analysis of the dominant eigenvalues obtained at Step 1. The poles can be chosen as following:
- poles whose frequency is close to re-assigned dominant closed-loop poles.
- poles corresponding to frequency domain properties (cut off frequency and so on)
- low frequency poles used to ensure precision (integral effect).
- At this stage, the coefficients a_{ijk} of transfer functions (Equation (6)) are all fixed. Note that in practice, the choice of the controller poles is not of primary importance, provided that the above recommendations are more or less taken into account.
- Eigenstructure assignment: the constraints defining the re-assignment of dominant eigenstructure (selected at Step 1) are derived; these constraints correspond to Equations (3) and (4). The number of constraints depends on the desired controller order. The higher the order, the higher the number of constraints to be processed. The equations for eigenstructure assignment are linear constraints. At this stage, using Proposition 2, Equation (8) ($\Xi A_1 = b_1$) is known.
- Controller structure constraints: the constraints relative to the gain structure are derived with the previous constraints. So, there is an additional equality constraint and new constraints of the form $\Xi A'_1 = b'_1$ are added.
- Criterion: a quadratic criterion of the form Equation (7) where $K_{ref}(s)$ is the transfer function of the initial controller is defined. This criterion will eventually fix the degrees of freedom remaining after the above constraints have been taken into account. The choice of the frequencies ωj depends on the frequency domain features of the initial controller. At this stage, using Proposition 2, the criterion is written in the following form: $J = \Xi H \Xi^T + 2\Xi c$
- Solve the LQP problem for Ξ , then deduce from Ξ the values of the coefficients b_{ijk}.

Step 3 – Final analysis

Performance can be evaluated in many ways:

- in the time domain, by means of step response simulations or root loci
- in the frequency domain, by means of Bode plots or singular value analysis
- in the parametric domain, by means of μ-analysis.

If some properties are not satisfactory, the procedure of Step 2 must be repeated till a satisfactory reduced controller is found.

When dealing with parametric robust controllers, Procedures 1 and 2 can be advantageously coupled. As long as degrees of freedom b_{ijk} are available, multi-model assignment can be performed in order to have a reduced controller robust to some parametric uncertainties. The design procedure for robustness improvement consists of applying the same procedure as in Step 2, with a single difference: the eigenstructure assignment constraints are now relative to several models.

2.5 Self-scheduling control

Classical gain-scheduling is typically done by interpolating a posteriori the linear controllers obtained for several models. But, because of structure, the gain-scheduling problem can be difficult to tackle and non-interpolability can occur[22,23]. Multi-model modal control handles this task by choosing a priori the interpolation formula for the controller gain. This choice can be guided by physical constraints, open-loop analysis and previous experiments. For example, let us take a scheduling with respect to measurable parameters (δ_1,δ_2) and an interpolation formula:

$$K_{sched}(s,\delta_1,\delta_2) = K_0(s)+\delta_1 K_{\delta 1}(s)+\delta_2 K_{\delta 2}(s) + \delta_1 \delta_2 K_{\delta 1 \delta 2}(s) \quad \ldots (9)$$

The synthesis of this controller can then be addressed by using the following Proposition 3[9].

Proposition 3. The determination of such a self-scheduled controller is equivalent to the synthesis of a multi-model modal controller

$$K_{dyn.eq}(s) = [K_0(s)\ \ K_{\delta 1}(s)\ \ K_{\delta 2}(s)\ \ K_{\delta 1 \delta 2}(s)] \quad \ldots (10)$$

with respect to the augmented system

$$\left[A(\Delta), B(\Delta), \begin{pmatrix} C(\Delta) \\ \delta_1 C(\Delta) \\ \delta_2 C(\Delta) \\ \delta_1\delta_2 C(\Delta) \end{pmatrix}, \begin{pmatrix} D(\Delta) \\ \delta_1 D(\Delta) \\ \delta_2 D(\Delta) \\ \delta_1\delta_2 D(\Delta) \end{pmatrix} \right] \quad \ldots (11)$$

Hence, it is sufficient to apply our multi-model design Procedure 1 on the augmented system (Equation (11)) for the controller $K_{dyn.eq}(s)$ and to extract from it the matrices $K_0(s)$, $K_{\delta 1}(s)$, $K_{\delta 2}(s)$ and $K_{\delta 1 \delta 2}(s)$ for the realisation of $K_{sched}(s, \delta_1,\delta_2)$. As demonstrated, the problem boils down to increasing the number of outputs of the original system ($A(\Delta)$,$B(\Delta)$,$C(\Delta)$,$D(\Delta)$) from p to $4p$. The augmentation of the ouput number offers additional degrees of freedom necessary for the simultaneous resolution of some linear constraints of type Equation (4). This led to many aeronautical and aerospace applications[10,24,25].

In conclusion, suppose now that some parameters of Δ are measurable and others are not. Using the procedures above, one could then self-schedule the controller with respect to the measurable parameters and use dynamic feedback to handle robustness with respect to non-measurable parameter variations. This will be applied on our problem at stake.

3.0 MODEL AND CONSTRAINTS

In this section, we describe the Challenger 604 aircraft longitudinal motion and the specifications to be fulfilled.

https://doi.org/10.1017/S000192400000556X Published online by Cambridge University Press

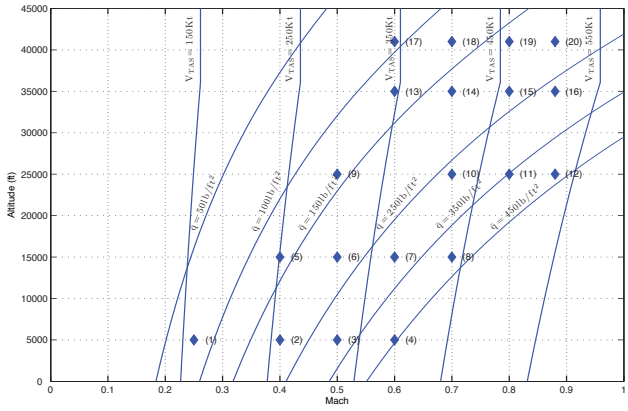


Figure 1. Flight envelope.

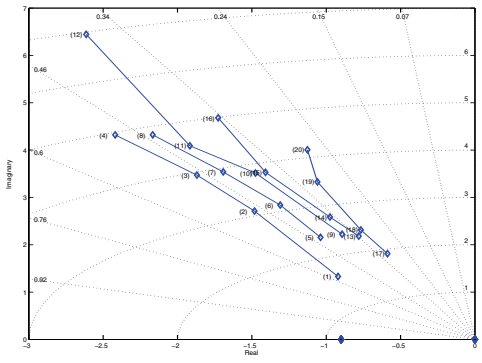


Figure 2. Open-loop short period pole dispersion.

3.1 Challenger 604 aircraft model

For design purposes, we consider the linearised short-period equations of motion.

$$\begin{bmatrix} \dot{w} \\ \dot{q} \\ \dot{\epsilon} \end{bmatrix} = \begin{bmatrix} Z_w & U_0 & Z_\epsilon \\ M_w & M_q & M_\epsilon \\ E_w & 0 & E_\epsilon \end{bmatrix} \begin{bmatrix} w \\ q \\ \epsilon \end{bmatrix} + \begin{bmatrix} Z_{\delta_e} \\ M_{\delta_e} \\ 0 \end{bmatrix} \delta_e \quad \ldots (12)$$

where the coefficients Z_w, Z_ϵ, M_w, M_q, M_ϵ, E_w, E_ϵ, Z_{δ_e}) and M_{δ_e})are stability derivatives calculated at each considered equilibrium point[26]. The state variable ϵ denotes the tail downwash angle[1]. The available measurements are pitch rate q and normal acceleration n_z:

$$\begin{bmatrix} q \\ n_z \end{bmatrix} = \begin{bmatrix} 0 & 1 & 0 \\ \tilde{Z}_w & \tilde{Z}_q & \tilde{Z}_\epsilon \end{bmatrix} \begin{bmatrix} w \\ q \\ \epsilon \end{bmatrix} + \begin{bmatrix} 0 \\ \tilde{Z}_{\delta_e} \end{bmatrix} \delta_e \quad \ldots (13)$$

where

$$n_z = (\dot{w} - U_0 q - l_x \dot{q})/g \quad \ldots (14)$$

so $\tilde{Z}_w$, $\tilde{Z}_q$, $\tilde{Z}_\epsilon$ and $\tilde{Z}_{\delta_e}$ can be deduced from the other coefficients. Twenty flight conditions and associated linearised models (defined by Mach number M and altitude h) were provided by Bombardier Inc. as illustrated in Fig. 1. Moreover, we consider complete actuator and IRU sensor dynamics such that the original open-loop order is 35; after balanced reduction[6], it is reduced to a 16th model in order to facilitate the H_∞ synthesis phase. Nevertheless, the reader must keep in mind that all time-responses will be performed on the original high-order system.

Figure 2 illustrates the open-loop short period pole dispersion over the flight envelope. The solid line indicates flight conditions with the same altitude. By observing, we can conclude that with increasing altitude, damping diminishes, and with increasing Mach, natural pulsation also increases.

Each flight condition is derived in eight configurations for different masses m and centres of gravity locations x_{cg} (Table 1).

Table 1
Grid points for varying m and x_{cg}

m(lbs)\ x_{cg} (% chord)	**16**	**20**	**35**	**38**	**48**
30,000		(1)	(2)		
32,000					(7)
39,000		(3)		(4)	(8)
46,000	(5)			(6)	

The system can then be rewritten as:

$$\dot{x} = A(\Delta)x + B(\Delta)u \quad \ldots (15)$$

$$y = C(\Delta)x + D(\Delta)u \quad \ldots (16)$$

where x is the state vector, y the measurement vector and u the input vector. The state-space matrices $A(\Delta)$, $B(\Delta)$, $C(\Delta)$, $D(\Delta)$ depend on the parameters (M,h,m,x_{cg}) described by the matrix Δ. We actually do not have an explicit formulation of the model in Δ but a bank of 160 models $\{M_j = (A_{\Delta j},B_{\Delta j},C_{\Delta j},D_{\Delta j}), j = 1\ldots 160\}$ for different values Δ_j of the parameters[2]. In the following, we will denote each model as Model $x.y$ with x the flight condition number (Fig. 1) and y the configuration number (Tab. 1). One could eventually find an LFT form by interpolating the data[27].

3.2 Handling quality requirements

The overall performance objective is to track pitch rate commands with predicted Level 1 handling qualities and desired time domain response behaviour. The handling quality criteria considered in this article are short period mode damping ratio ζ_{sp}, Gibson's dropback Drb (see Appendix A), settling time ST, pitch attitude bandwidth $\omega_{BW\theta}$), and phase delay τ_p[28]. The boundaries of these criteria are defined by military standards[29]. Even though handling qualities are primarily defined for military aircraft, they are usually applied to commercial aircraft with slight modifications, derived from the manufacturer's experience. Table 2 summarises the handling quality boundaries being considered in the design procedure.

Table 2
Handling qualities

Handling qualities	**Level 1**
Short Period damping ζ_{sp}	$0{\cdot}35 \leq \zeta_{sp}$
θ-bandwith $\omega_{BW\theta}$	$\omega_{(BW\theta)} \geq 1{\cdot}5$ (rad/s)
Gibson's dropback Drb	$-0{\cdot}2 \leq Drb \leq 0{\cdot}5$
Phase delay τ_p	$\tau_p \leq 0{\cdot}2$(s)
Settling time ST	2% en 3(s)

4.0 APPLICATION TO THE LONGITUDINAL FLIGHT CONTROL PROBLEM

We seek a controller which satisfies the handling quality requirements over the entire flight envelope and is robust to mass m and centre of gravity x_{cg} variation; consequently, the controller will be scheduled with respect to dynamic pressure $\bar{q}$ and altitude h while presenting good parametric robustness with respect to m and x_{cg}. Moreover its order must be as low as possible. The theoretical background presented in Section 2 suggests the methodology we now propose:

Step 1 Compute H_∞ controllers satisfying handling qualities on different flight conditions with good parametric robustness.

https://doi.org/10.1017/S000192400000556X Published online by Cambridge University Press

Step 2 Reduce these controllers with the technique presented in Section 2.4. Performance must be preserved and low order controllers with similar structure should be obtained.

Step 3 Schedule these reduced controllers with the self-scheduling technique presented in Section 2.5.

4.1 H_∞ synthesis

For a given flight condition, we seek an initial controller that satisfies the handling quality requirements for the eight configurations. H_∞ synthesis is a good candidate to obtain such a controller. Zames[4] initiated this theory, which was further developed by Doyle[30]. The H_∞ problem is a stabilisation and disturbance rejection problem. We must search for a controller that will minimise disturbance effects while stabilising the system. Theoretical aspect can be found in Zhou *et al*[31] and Alazard *et al*[32].

Let us consider the augmented system $P(s)$ (including weight functions or filters) composed by four multivariable transfer functions between the inputs u and w and the outputs y and z where:

- u represents the system command
- w represents exogenous inputs (reference and/or disturbance)
- y represents measurements
- z represents regulated outputs

$P(s)$ can be separated in the following way:

$$\begin{bmatrix} Z(s) \\ Y(s) \end{bmatrix} = \begin{bmatrix} P_{11}(s) & P_{12}(s) \\ P_{21}(s) & P_{22}(s) \end{bmatrix} \begin{bmatrix} W(s) \\ U(s) \end{bmatrix} \quad \ldots (17)$$

By closing the loop with the control law $U(s) = K(s)Y(s)$, one can obtain the transfer between the inputs w and the outputs z namely Linear Fractionnal Transformation (LFT):

$$G_{zw}(s) = F_l(P(s), K(s)) = P_{11} + P_{12}K(s)(I - P_{22}K(s))^{-1}P_{21} \quad \ldots (18)$$

The optimal H_∞ problem is the synthesis of a controller $K(s)$ among all internally stabilising controllers that minimises the H_∞ norm of $G_{zw}(s) = F_l(P(s),K(s))$. We remind that the H_∞ norm of a transfer function $G(s)$ is defined as:

$$\|G(s)\|_\infty = \sup_{\omega \in \mathbb{R}} \bar{\sigma}(G(j\omega)) \quad \ldots (19)$$

Optimal H_∞ problem

Finding a stabilising controller $K(s)$ *such as* $\|F_l(P(s), K(s))\|_\infty$ *is minimal.*

Knowing the minimal H_∞ norm can be theoretically useful because a limit can be fixed on the reachable performances. Nevertheless, in a practical way, the suboptimal H_∞ problem is defined where the H_∞ norm is reduced under a positive threshold γ.

Suboptimal H_∞ problem

Finding a stabilising controller $K(s)$ such as $\|F_l(P(s), K(s))\|_\infty \leq \gamma$. Although there are several ways to solve this problem, the Doyle *et al*[5] method will be used as it is based upon a state variable approach. The augmented plant considered for the H_∞ synthesis is given in Fig. 5.

In order to produce an efficient H_∞ controller, a reference model that satisfies the constraints is chosen:

$$F_{\text{ref}}(s) = \frac{e^{-0.1s}(0.66s+1)}{s^2+2(0.7)(2.5)s+(2.5)^2} \quad \ldots (20)$$

The difference between the reference model output and the aircraft pitch rate q is weighted by a low-pass filter W_{perf}:

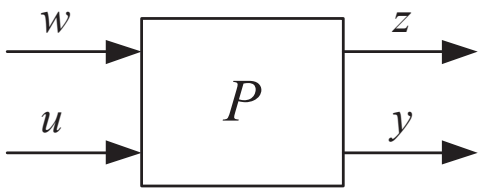


Figure 3. Augmented model.

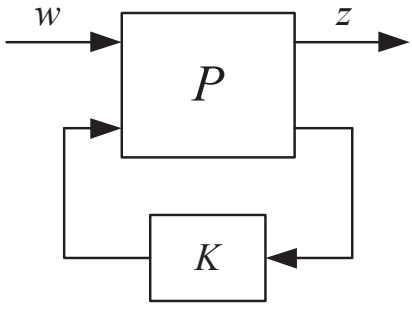


Figure 4. Standard H_∞ synthesis.

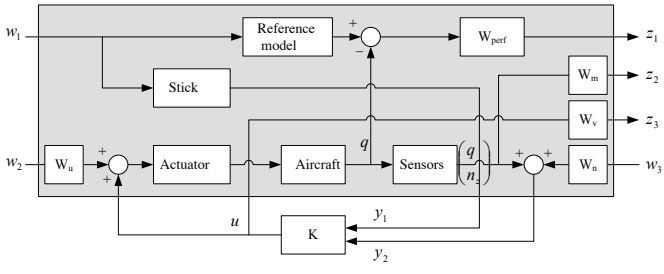


Figure 5. H_∞ synthesis diagram.

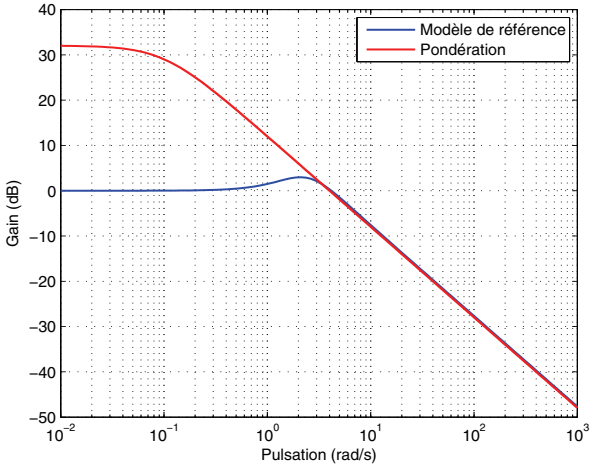


Figure 6. Reference model and error model weighting.

https://doi.org/10.1017/S000192400000556X Published online by Cambridge University Press

$$W_{perf}(S) = \frac{40}{10s+1} \quad \ldots (21)$$

As shown in Fig. 6, low-frequencies are highly weighted by the gain factor, and the filter time constant is consequently chosen to cover the bandwidth of interest on which the model matching is sought.

In order to limit controller bandwidth and ensure roll-off constraints, we use a second order high-pass filter on the command input:

$$W_v(s) = 0{\cdot}1\left(\frac{s/15+1}{s/1000+1}\right)^2 \quad \ldots (22)$$

Additional inputs/outputs and associated weightings ($W_u = 0{\cdot}5$, $W_n = 0{\cdot}03I_2$, W_m = diag(0·03, 0·01)) are complementary sensitivity functions to improve robustness. These weights and filters have been elected after some trials/errors to adequately shape the time-responses and the characteristics. Finally a 23rd order controller is obtained which ensures satisfactory time-responses for all configurations (Fig. 7). As indicated by Table 3 handling quality constraints are reasonably well satisfied.

Table 3
Handling quality values of the H_∞ controller

Model	ζ_{sp}	$\omega_{BW\theta}$	*Drb*	τ_p	ST
Model 1.1	0·64	1·5	0·02	0·23	1·69
Model 1.2	0·73	1·64	0·05	0·21	1·94
Model 1.3	0·60	1·4	0·03	0·22	1·78
Model 1.4	0·68	1·52	0·10	0·21	2·78
Model 1.5	0·54	1·32	–0·20	0·20	3·22
Model 1.6	0·66	1·51	0·20	0·21	3·21
Model 1.7	0·72	1·82	0·22	0·25	2·31
Model 1.8	0·66	1·66	0·25	0·24	2·52

4.2 Controller reduction using modal multi-model approach

The initial H_∞ controller order is 23. Before proceeding to the modal analysis, we will seek to significantly reduce the order of the controller by using balanced reduction techniques[6]. Moreover, as the controller is a two degree controller, the feedforward part is separated from the feedback part. Again, balanced reduction is performed on each sub-controller. Since we only have interest in the modal reduction in the feedback controller, the feedforward controller will remain as it was after the balanced reduction. Fortunately, the feedforward controller order is five without any major loss on the temporal, frequency and parametric criteria. One could remark actually that the poles of the feedforward path are the reference model poles and the integrator pole. The feedback controller order is reduced to 12 without any significant performance loss. If further balanced reduction is performed, there is some significant loss compared to the initial H_∞ controller. Modal reduction is used to further reduce the controller order if possible.

4.2.1 Modal analysis

First, a modal analysis is performed to find the dominant poles that must be re-assigned, and the poles that must be conserved in the feedback controller. We find that the poles of interest are:

- the integrator pole of the controller,
- the short period mode poles,
- the complex poles –6·21± 17·98*i* of the controller

After some trials, we finally choose the poles gathered in Table 4 for our controller.

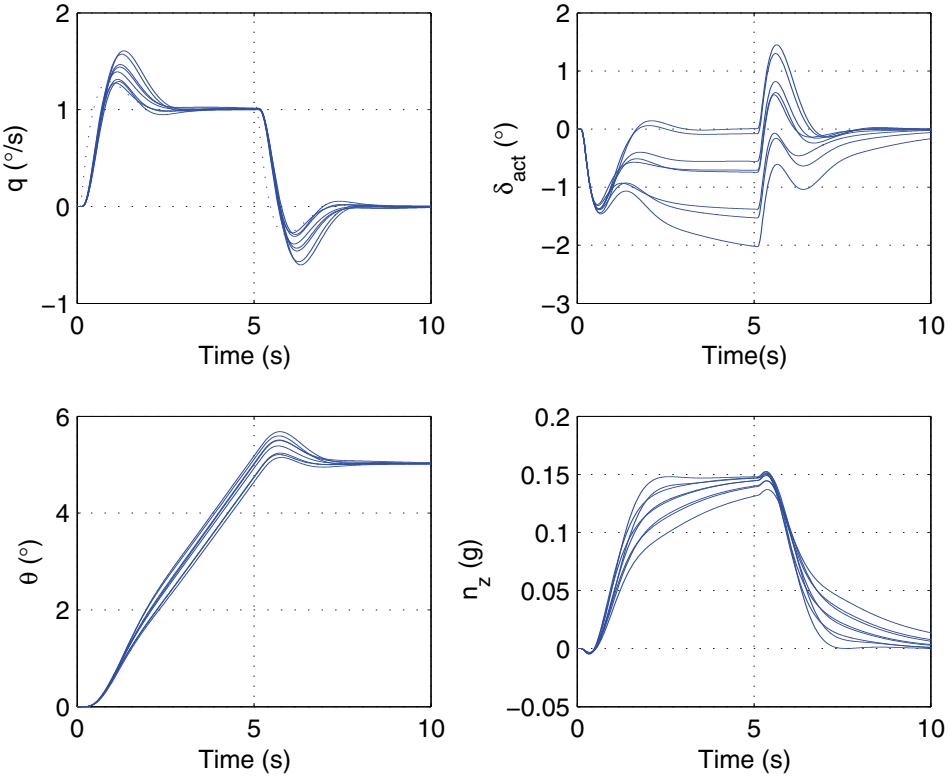


Figure 7. Time-responses of the H_∞ controller for Models 1.*y*.

https://doi.org/10.1017/S000192400000556X Published online by Cambridge University Press

Table 4
Reduced controller poles

Pole	Value
λ_1	0
λ_2	–0·835
λ_3	–6·21 ± 17·98*i*

4.2.2 First reduction

We first seek a reduced controller with structure in Table 5. We will not impose any degree difference. Our goal is to check that a 4th order controller can be used to preserve the performance of the original H_∞ controller. The eigenvalue assignment is completed on both models 1.1 and 1.5 (Table 6). Results are not presented as they are exactly similar to H_∞ controller results. The reduction is efficient.

Table 5
First reduced controller structure

Output	q	n_z
Poles	$\lambda_1\ \lambda_2\ \lambda_3$	$\lambda_1\ \lambda_2\ \lambda_3$
Degree difference	0	0

Table 6
Placement constraints for first reduction

Model	Mode	Open-loop pole		Closed-loop pole
Model 1.1	Integrator	0	→	–0·74
Model 1.1	Short Period	–0·92 ± 1·33*i*	→	–3·33 ± 3·95*i*
Model 1.1	Corrector	–6·21 ± 17·98*i*	→	–14·88 ± 22·28*i*
Model 1.5	Integrator	0	→	–0·49
Model 1.5	Short Period	–0·68 ± 1·31*i*	→	–1·99 ± 3·10*i*
Model 1.5	Corrector	–6·21 ± 17·98*i*	→	–13·97 ± 18·33*i*

4.2.3 Second reduction

After the successful first reduction, we seek to structure our controller. The two feedback paths have originally integral action; we choose to keep the integral effect only on the q feedback. Moreover, to ensure some 'roll-off', we impose the degrees of the numerators as shown in Table 7. With fewer degrees of freedom, some constraints of Table 6 have to be abandoned. Consequently, we are not able to find a satisfactory reduced controller. After analysis, a constraint has to be added on Model 1.8 (Table 8).

Table 7
Second reduced controller structure

Output	q	n_z
Poles	$\lambda_1\ \lambda_2\ \lambda_3$	$\lambda_1\ \lambda_2$
Degree difference	1	2

Table 8
Placement constraints for second reduction

Model	Mode	Open-loop pole		Closed-loop pole
Model 1.1	Integrator	0	→	–0·74
Model 1.1	Corrector	–6·21 ± 17·98*i*	→	–14·88 ± 22·28*i*
Model 1.5	Short Period	–0·68 ± 1·31*i*	→	–1·99 ± 3·10*i*
Model 1.8	Integrator	0	→	–0·89

The reduced controller is then tested on the complete high order model, which is found to provide similar results to the original model concerning time-responses (Fig. 8). Table 9 summarises the handling quality values. These data are very close to the ones obtained with the original H_∞ controller. We finally managed to find a reduced controller that is still satisfactory.

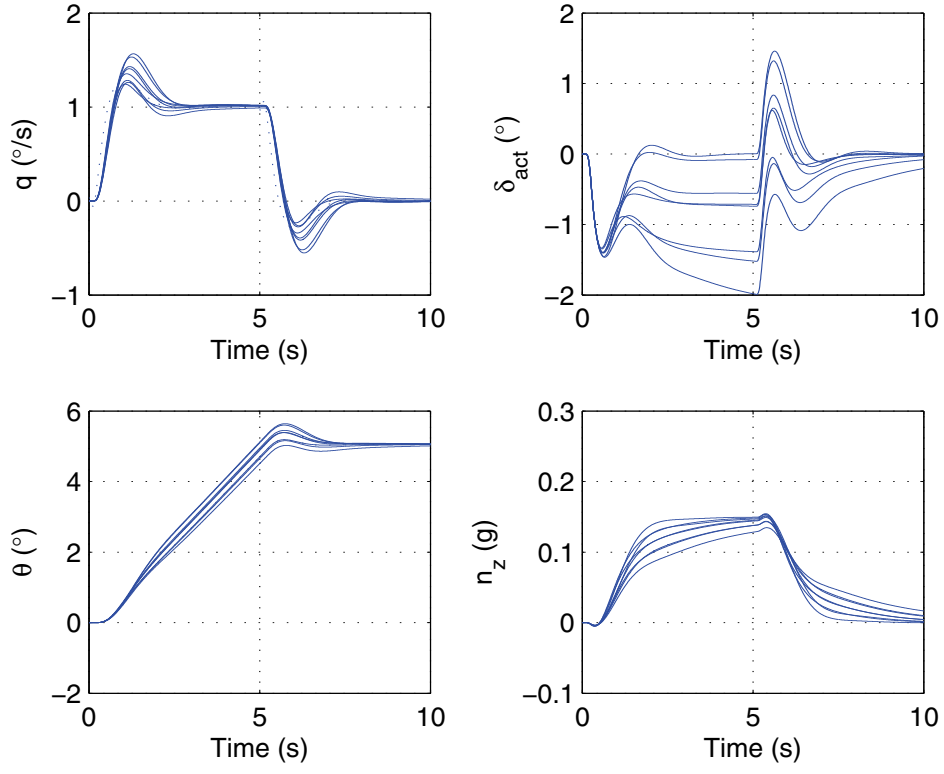


Figure 8. Time-responses of the final reduced H_∞ controller for Models 1.*y*.

https://doi.org/10.1017/S000192400000556X Published online by Cambridge University Press

Table 9
Handling quality values with the final reduced H_∞ controller

Model	ζ_{sp}	ω_{BW_θ}	*Drb*	τ_p	*ST*
Model 1.1	0·65	1·49	–0·04	0·23	2·39
Model 1.2	0·72	1·6	–0·06	0·21	2·94
Model 1.3	0·60	1·42	–0·01	0·22	2·78
Model 1.4	0·68	1·50	0·10	0·21	2·98
Model 1.5	0·54	1·30	–0·20	0·20	3·22
Model 1.6	0·66	1·50	0·18	0·21	3·21
Model 1.7	0·72	1·79	0·22	0·25	2·81
Model 1.8	0·66	1·66	0·19	0·24	2·72

4.3 Self-scheduled controller

The next step is to apply the self-scheduling technique (Section 2.5) to our problem at hand. As the flight envelope is expressed in terms of Mach number M and altitude h, these two measures are good candidates for scheduling parameters. Nevertheless, we propose to use dynamic pressure $\bar{q}$ instead of M^3. As the flight envelope is relatively large (Fig. 1), the design of the self-scheduling controller is made in two steps. We first establish a controller scheduled with respect to $\bar{q}$ at the lowest altitude of 5,000ft, then we extend the controller to the complete flight envelope by adding altitude h dependency in the controller.

4.3.1 Choice of structure

Our controllers can be reduced efficiently while still keeping good performance properties. Moreover, a common structure has been derived. Many choices can be made for the structure of the transfer functions $K_\delta(s)$. In order to maintain an order as low as possible for our controller, all denominators will be chosen equal for every $K_\delta(s)$. The H_∞ controllers do not necessarily have the same poles, which is a major inconvenience when interpolation of these controllers needs to be performed. Nevertheless, a similar structure has been found for the different reduced controllers; consequently, average values of the poles are chosen (Table 10). The low-frequency pole used in the reduction phase is replaced by a pole located at –20 and the complex poles $-10 \pm 25i$ is an average value of the different corresponding controller poles.

Table 10
Scheduled controller poles

Pole	Value
λ_1	0
λ_2	$-10 \pm 25i$
λ_3	–20

4.3.2 Initial controller synthesis

We will first work on the flight condition 1. The controller structure is given in Table 11 and the pole placement constraints are gathered in Table 12. This initial placement is similar to the one used in the final reduced controller. Time-responses remain similar to the ones obtained with the reduced controller of previous section (Fig. 8).

Table 11
Structure of the initial controller for self-scheduling

Output	q	n_z
Poles	$\lambda_1\lambda_2\lambda_3$	$\lambda_1\lambda_2$
Degree difference	1	2

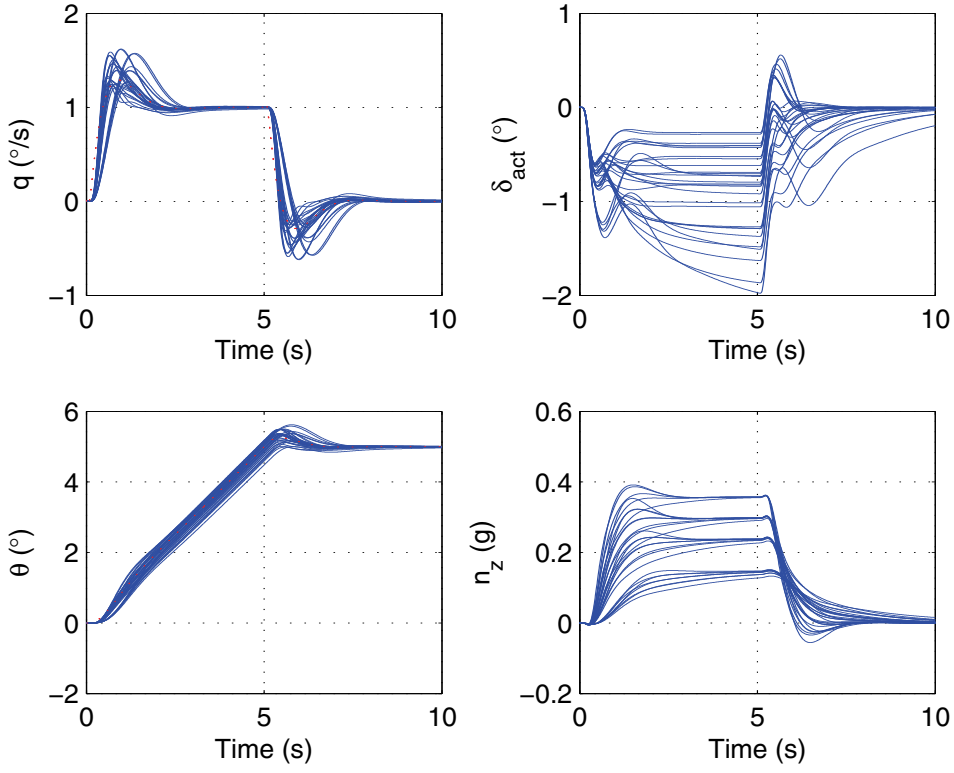


Figure 9. Time-responses with K(s,δq̄) for Models 1.y to 4.y.

https://doi.org/10.1017/S000192400000556X Published online by Cambridge University Press

Table 12
Placement constraint for initial controller $K_0(s)$

Model	Mode	Open-loop pole		Closed-loop pole
Model 1.1	Integrator	0	→	–0·74
Model 1.1	Corrector	$-10 \pm 25i$	→	$-14{\cdot}88 \pm 22{\cdot}28i$
Model 1.5	Short Period	$-0{\cdot}68 \pm 1{\cdot}31i$	→	$-1{\cdot}99 \pm 3{\cdot}10i$
Model 1.8	Integrator	0	→	–0·89

4.3.3 *Self-scheduled controller synthesis with respect to q at h = 5,000ft*

We first look for a scheduled controller with respect to $\bar{q}$ at the lowest altitude h = 5,000ft . The flight conditions to consider are 1 to 4. A quadratic scheduling is chosen:

$$K(s,\delta\bar{q}) = K_0(s) + \delta\bar{q}K_{\bar{q}}(s) + \delta\bar{q}^2 K_{\bar{q}^2}(s) \quad \ldots (23)$$

The dynamic pressure of flight condition one is the lowest of the flight envelope (77·1lb/ft^2), whereas the one of flight condition four is the highest (444·3lb/ft^2). The synthesis of the self-scheduled controller $K(s,\delta\bar{q})$ is done by placing the eigenstructure of the augmented system:

$$\left[A(\Delta), B(\Delta), \begin{pmatrix} C(\Delta) \\ \delta\bar{q}C(\Delta) \\ \delta\bar{q}^2 C(\Delta) \end{pmatrix}, \begin{pmatrix} D(\Delta) \\ \delta\bar{q}D(\Delta) \\ \delta\bar{q}^2 D(\Delta) \end{pmatrix}\right] \quad \ldots (24)$$

And the controller $K(s,\delta\bar{q})$ is calculated in the following way:

$$K(s,\delta\bar{q}) = [K_0(s) \;\; K_{\bar{q}}(s) \;\; K_{\bar{q}^2}(s)] \quad \ldots (25)$$

The same structure is preserved for $K_{\bar{q}}(s)$ and $K_{\bar{q}^2}(s)$ (Table 11).

Multimodel synthesis

We maintain the placement of Model 1 (Table 12) and add placement constraints on Models 3 and 4 (Table 13). We essentially place short period and integrator modes. The different configurations are chosen according to the observations made on H_∞ controller reduction. Moreover, one controller pole has to be placed on Model 4.1.

Table 13
Additional constraints for scheduled controller $K(s,\delta\bar{q})$

Model	Mode	Open-loop pole		Closed-loop pole
Model 3.1	Short Period	$-1{\cdot}87 \pm 3{\cdot}47i$	→	$-{\cdot}23 \pm 6{\cdot}2i$
Model 3.5	Integrator	0	→	–0·72
Model 3.7	Integrator	0	→	–1·51
Model 3.7	Short Period	$-1{\cdot}68 \pm 1{\cdot}46i$	→	$3{\cdot}58 \pm 2{\cdot}08i$
Model 4.1	Integrator	0	→	–1·99
Model 4.1	Corrector	$-10 \pm 25i$	→	$1{\cdot}42 \pm 26{\cdot}09i$
Model 4.5	Integrator	0	→	–0·97
Model 4.5	Short Period	$-1{\cdot}78 \pm 4{\cdot}11i$	→	$-3{\cdot}67 \pm 4{\cdot}51i$

Analysis

The time-responses of Models 1 to 4 (for the 8 configurations) are illustrated in Fig. 9. A good temporal behaviour is preserved, similar to the one observed with H_∞ controller. Although, placement constraints are only applied on Models 1, 3 and 4, one can see that Model 2 (and its different configurations) exhibits the expected behaviour.

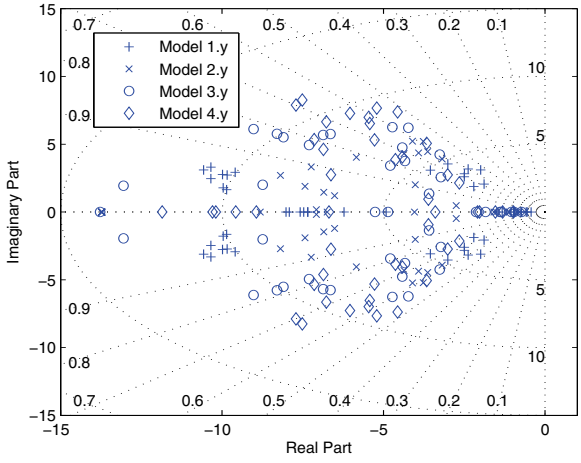


Figure 10. Pole map with $K(s,\delta\bar{q})$ for Models 1.*y* to 4.*y*.

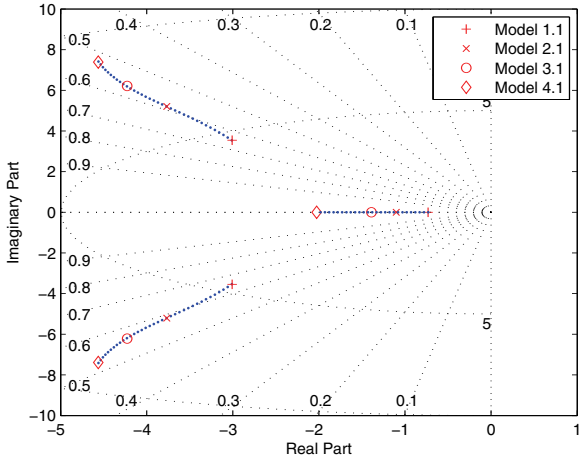


Figure 11. Short Period evolution with $K(s,\delta\bar{q})$ for M ∈ [0·25,0·6] and h = 5000ft (Models x.1).

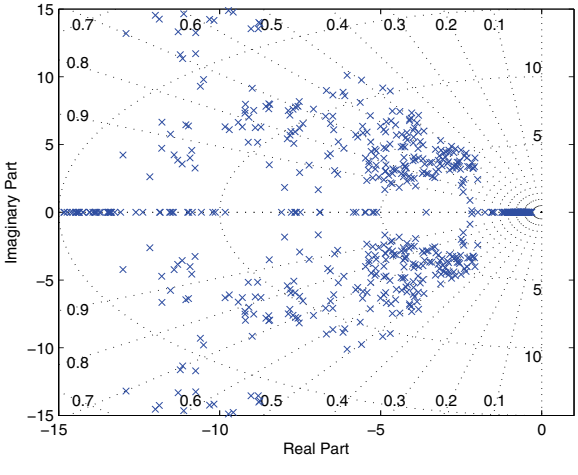


Figure 12. Pole map with $K(s,\delta\bar{q},\delta h)$ for the 160 models.

https://doi.org/10.1017/S000192400000556X Published online by Cambridge University Press

On the pole map (Fig. 10) all low frequency poles have a damping ratio greater than 0·5; poles issued from the integrator have a real part less than –0·5.

By using the parametric model in M and h, we validate the closed-loop pole evolution (essentially short period mode) for M ∈ [0·25, 0·6] and h = 5,000ft. Figure 11 shows that for the nominal configuration (Models 1.1 to 4.1), short period mode evolves smoothly with an increasing natural frequency as M grows and a damping ratio between 0·55 and 0·65.

4.3.4 Self-scheduled controller synthesis w.r.t. $\bar{q}$ and h

If we plot the time-responses with controller $K(s,\bar{q})$ on the set of 160 models, they are not as good as expected. Nevertheless, the system remains stable for all configurations and closed-loop poles have a damping ratio greater than 0·3. Adding new scheduled terms in $\bar{q}^3$ and $\bar{q}^4$ do not improve the results, so we decide to use a second scheduling variable h to take into account the change of altitude. We gradually add terms in h, $\bar{q}h$, h^2... while checking performance on the entire flight envelope. We finally decide to use a self-scheduled controller of the form:

$$K(s,\delta\bar{q},\delta h) = K_0(s) + \delta\bar{q}K_{\bar{q}}(s) + \delta\bar{q}^2K_{\bar{q}^2}(s) + \delta hK_h(s) + \delta h^2K_{h^2}(s) + \delta\bar{q}\delta hK_{\bar{q}h}(s) \quad \ldots (26)$$

The synthesis of the self-scheduled controller $K(s,\delta\bar{q},\delta h)$ is done by placing the eigenstructure of the augmented system:

$$\left[A(\Delta), B(\Delta), \begin{pmatrix} C(\Delta) \\ \delta\bar{q}C(\Delta) \\ \delta\bar{q}^2C(\Delta) \\ \delta hC(\Delta) \\ \delta h^2C(\Delta) \\ \delta\bar{q}\delta hC(\Delta) \end{pmatrix}, \begin{pmatrix} D(\Delta) \\ \delta\bar{q}D(\Delta) \\ \delta\bar{q}^2D(\Delta) \\ \delta hD(\Delta) \\ \delta h^2D(\Delta) \\ \delta\bar{q}\delta hD(\Delta) \end{pmatrix}\right] \quad \ldots (27)$$

And the controller $K(s,\delta\bar{q},\delta h)$ is calculated in the following way:

$$K(s,\delta\bar{q},\delta h) = [K_0(s)\ K_{\bar{q}}(s)\ K_{\bar{q}^2}(s)\ K_h(s)\ K_{h^2}(s)\ K_{\bar{q}h}(s)] \quad \ldots (28)$$

As before, the structures of $K_h(s)$, $K_{h^2}(s)$ and $K_{\bar{q}h}(s)$ are the ones exposed in Table 11. We start from the controller $K(s,\delta\bar{q})$ and keep the placement constraints.

Multi-model synthesis

Additional constraints were deduced on the following observations:

- worst damped poles ($\zeta < 0{\cdot}4$) with $K(s,\delta\bar{q})$ are those of Models 16 and 20 (high altitudes h = 35,000ft and h = 42,000ft and M = 0·88).
- thanks to reduction phases, we know on which Models 16.y and 20.y to operate.
- Table 14 gathers the additional constraints.

Analysis

Figure 12 shows the closed-loop poles on the 160 models with controller $K(s,\delta\bar{q},\delta h)$. Short period mode poles have damping ratio greater than 0·5 (with a few exceptions). Time-responses of Fig. 13 are all satisfactory on the entire set of models. The self-scheduled controller $K(s,\delta\bar{q},\delta h)$ ensures good performance on the entire flight envelope and is robust for the different mass/centre of gravity configurations.

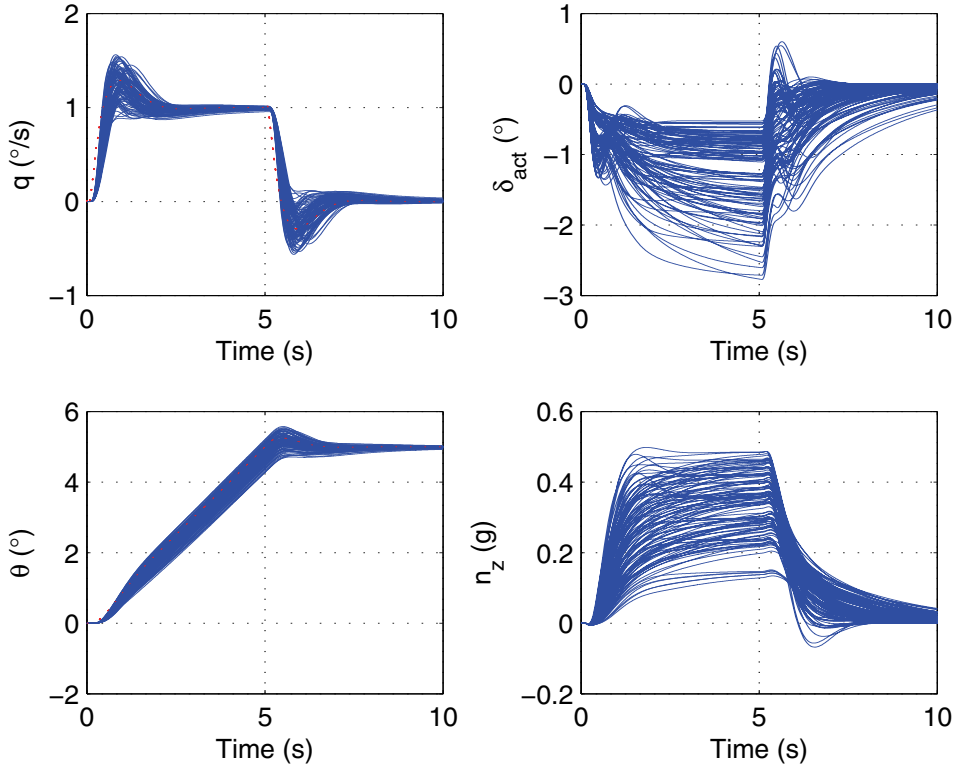


Figure 13. Time-responses with $K(s,\delta\bar{q},\delta h)$ for the 160 models.

https://doi.org/10.1017/S000192400000556X Published online by Cambridge University Press

Table 14
Additional constraints for scheduled controllers $K(s,\delta\bar{q},\delta\bar{h})$

Model	Mode	Open-loop pole		Closed-loop pole
Model 12.1	Short Period	$-2{\cdot}61 \pm 6{\cdot}44i$	→	$-5{\cdot}52 \pm 7{\cdot}07i$
Model 12.5	Integrator	0	→	$-1{\cdot}25$
Model 12.5	Short Period	$-1{\cdot}88 \pm 5{\cdot}58i$	→	$-3{\cdot}91 \pm 5{\cdot}48i$
Model 12.7	Short Period	$-2{\cdot}37 \pm 3{\cdot}38i$	→	$-2{\cdot}54 \pm 3{\cdot}82i$
Model 16.1	Corrector	$-10 \pm 25i$	→	$-10{\cdot}28 \pm 28{\cdot}21i$
Model 16.5	Integrator	0	→	$-0{\cdot}68$
Model 16.5	Short Period	$-1{\cdot}09 \pm 4{\cdot}14i$	→	$-3{\cdot}64 \pm 7{\cdot}36i$
Model 16.7	Short Period	$-1{\cdot}56 \pm 1{\cdot}75i$	→	$-2{\cdot}44 \pm 2{\cdot}90i$
Model 17.1	Integrator	0	→	$-0{\cdot}52$
Model 17.1	Short Period	$-0{\cdot}58 \pm 1{\cdot}82i$	→	$-3{\cdot}86 \pm 7{\cdot}07i$
Model 17.5	Short Period	$-0{\cdot}43 \pm 1{\cdot}74i$	→	$-2{\cdot}70 \pm 4{\cdot}58i$
Model 17.7	Short Period	$-1{\cdot}03$ and $-0{\cdot}11$	→	$-3{\cdot}80 \pm 3{\cdot}82i$
Model 20.1	Integrator	0	→	$-0{\cdot}98$
Model 20.5	Integrator	0	→	$-0{\cdot}85$
Model 20.5	Short Period	$-0{\cdot}72 \pm 3{\cdot}38i$	→	$-2{\cdot}64 \pm 5{\cdot}44i$
Model 20.7	Short Period	$-1{\cdot}01 \pm 2{\cdot}27i$	→	$-1{\cdot}96 \pm 1{\cdot}82i$

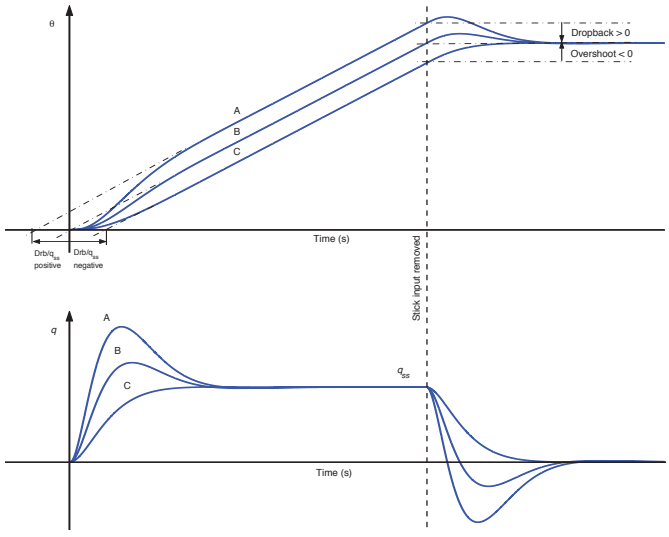


Figure 14. Gibson's dropback definition.

5.0 CONCLUSION

The complete design of the longitudinal flight controller of a Challenger 604 has been carried out. Based on a reference model satisfying many handling qualities, we were able to design effective high-order controllers using H_∞ synthesis working with different flight conditions. The controllers presented robust performance versus mass and centre of gravity variations. Robust modal reduction was then performed on these controllers to significantly lower their order, while still preserving performance and imposing a common structure. Finally, a self-scheduling technique allowed us to schedule the gains with respect to dynamic pressure and altitude over the entire flight envelope. The final product is an efficient 4th order scheduled controller that is robust to mass and centre of gravity variations, satisfying most of the handling qualities considered.

APPENDIX

Dropback

Besides the classical time-domain criteria such as settling time, overshoot or rising time, Gibson's dropback is commonly used by flight control engineers. This short term measure of the pitch attitude changes is calculated based on the reduced-order attitude θ response (i.e. without the Phugoid mode) to a stick step input removed after a few seconds. Figure 14 illustrates how to calculate the dropback *Drb*. The quantity q_{ss} is the pitch rate steady state value. Ideally, having a zero dropback value means piloting a pure integrator in θ after a short time. As it is preferred to have positive dropback values instead of negative ones, this comes with some significant overshoots in the pitch rate *q* response.

REFERENCES

1. HYDE, R.A. *H_∞ Aerospace Control Design – A VSTOL Flight Application*, 1996, Springer, New York, USA.
2. TISCHLER, M.B. *Advances in Aircraft Flight Control*, 1996, Taylor & Francis Ltd, London, UK.
3. GAUTREY, J.E. *Flying Qualities and Flight Control System Design for a Fly-by-Wire Transport Aircraft*, 1998, PhD thesis, Cranfield University, College of Aeronautics.
4. ZAMES, G. Feedback and optimal sensitivity: Model reference transformations, multiplicative seminorms, and approximations, *IEEE Transactions on Automatic Control*, 1989, **26**, (2), pp 301–320.
5. DOYLE, J.C., GLOVER, K., KHARGONEKAR, P.P. and FRANCIS, B.A. State-space solutions to standard H_2 and H_∞ control problems, *IEEE Transactions on Automatic Control*, 1989, **34**, (8), pp 831–847.
6. OBINATA, G. and ANDERSON, B.D.O. *Model Reduction for Control System Design*, 2001, Springer, New York, USA.
7. CHABLE, S., MATHIEU, S. and CHIAPPA, C. Design and optimisation of restricted complexity controller: A modal approach for reduced-order controllers, *European J Control*, 2003, **9**, (1), pp 39–47.
8. LE GORREC, Y., MAGNI, J.F., DÖLL, C. and CHIAPPA, C. A modal multi-model control design approach applied to aircraft autopilot design, *AIAA J Guidance, Control and Dynamics*, 1998, **21**, (1), pp 77–83.
9. MAGNI, J.F. *Robust Modal Control with a Toolbox for use with Matlab®*, 2002, Springer.
10. DÖLL, C., LE GORREC, Y., FERRERES, G. and MAGNI, J.F. A robust self-scheduled missile autopilot: Design by multi-model eigenstructure assignment, *Control Engineering Practice*, October 2001, **9**, (10), pp 1067–1078.
11. LEITH, D.J. and LEITHEAD, W.E. Survey of gain-scheduling analysis and design, *Int J Control*, 2000, **73**, (11), pp 1001–1025.
12. RUGH, W.J. and SHAMMA, J.S. Research on gain-scheduling, *Automatica*, October 2000, **36**, (10), pp 1401–1425.
13. LE GORREC, Y. Commande Modal Robuste et Synthèse de Gains Autoséquencés. Approche Multimodèle, 1998, PhD thesis, École Nationale Supérieure de l'Aéronautique et de l'Espace.
14. MOORE, B.C. On the flexibility offered by state feedback in multivariable system beyond closed loop eigenvalue assignment, *IEEE Transactions on Automatic Control*, 1976, **21**, pp 659–692.
15. MAGNI, J. F., LE GORREC, Y. and CHIAPPA, C. A multimodel-based approach to robust and self-scheduled control design, 37th IEEE Conference on Decision and Control, Tampa, Florida, USA, 1998, pp 3009–3014.
16. KALMAN, R.E., HO, Y.C. and NARENDRA, K.S. Controllability of linear dynamic systems, *Contributions to Differential Equations*, 1963, **1**, (2), pp 189-213.
17. DOYLE, J.C., LENZ, K. and PACKARD, A. Design examples using μ-synthesis: Space shuttle lateral axis FCSduring re-entry, 25rd IEEE Conference on Decision and Control, Athens, Greece, 1986, pp 2218–2223.
18. PACKARD, A. and DOYLE, J.C. The complex structured singular value, *Automatica*, January 1993, **29**, (1), pp 71–109.
19. MAGNI, J.F. and DÖLL, C. A new lower bound of the mixed structured singular value, Proc. 2nd Asian Control Conference, Seoul, South Korea, 1997, **I**, pp 847–850.

https://doi.org/10.1017/S000192400000556X Published online by Cambridge University Press

20. MAGNI, J.F. Multimodel eigenstructure assignment in flight control design, *Aerospace Sciences and Technologies*, 1999, **3**, (3), pp 141–151.
21. CHIAPPA, C., MAGNI, J.F., DÖLL, C. and LE GORREC, Y. Improvement of the robustness of an aircraft autopilot designed by an H_∞ technique, Procedures of the CESA'98 Conference, 1998, pp 1016–1020.
22. LAWRENCE, D.A. and RUGH, W.J. Gain scheduling dynamic linear controllers for a nonlinear plant, *Automatica*, March 1995, **31**, (3), pp 381–390.
23. STILWELL, D.J. and RUGH, W.J. Stability preserving interpolation methods for the synthesis of gain-scheduled controllers, *Automatica*, 2000, **33**, (7), pp 1263–1271.
24. CONSTANT, G., CHABLE, S., CHIAPPA, C. and DÖLL, C. Robustification of an H_2 autopilot for flexible aircraftby self scheduling based on multi model eigenstructure assignment, International Council of Aeronautical Sciences, 2002, pp 542.1–542.9.
25. SAUSSIÉ, D., SAYDY, L. and AKHRIF, O. Gain scheduling control design for a pitch-axis missile autopilot, AIAA Guidance, Navigation and Control Conference and Exhibit, Honolulu, USA, 2008.
26. NELSON, R.C. *Flight Stability and Automatic Control,* 2nd edition, 1998, WCB/McGrawHill, Boston, USA.
27. MAGNI, J.F. User manuel of the linear fractional representation toolbox, version 2.0, Technical report, CERT – DCSD, 2005.
28. SAUSSIÉ, D., SAYDY, L. and AKHRIF, O. Longitudinal flight control design with handling quality requirements, *Aeronaut J*, 2006, **110**, (1111), pp 627–637.
29. US Department of Defence, Flying qualities of piloted aircraft, MIL-HDBK-1797A, 1997, Government Printing Office, Washington DC, USA.
30. DOYLE, J.C. Analysis of feedback systems with structured uncertainty, IEE Proceedings, Part D, 1982, **129**, pp 242–250.
31. ZHOU, K. and DOYLE, J.C. *Essentials of robust control*, 1998, Prentice Hall, Upper Saddle River, NJ, USA.
32. ALAZARD, D., CUMER, C., APKARIAN, P., GAUVRIT, M. and FERRERES, G., Robustesse et commande optimale, 1999, Cepadues-Editions, Toulouse, France.

https://doi.org/10.1017/S000192400000556X Published online by Cambridge University Press